**Wind and Structures**, *Vol. 18, No. 1 (2014) 001-020*
DOI: http://dx.doi.org/10.12989/was.2014.18.1.001 

# Refined optimal passive control of buffeting-induced wind loading of a suspension bridge

M. Domaneschi* and L. Martinelli[a]

*Department of Civil and Environmental Engineering, Politecnico di Milano, Milano Italy*

*(Received November 24, 2012, Revised July 25, 2013, Accepted August 19, 2013)*

**Abstract.** Modern design of long suspension bridges must satisfy at the same time spanning very long distances and limiting their response against several external loads, even if of high intensity. Structural Control, with the solutions it provides, can offer a reliable contribution to limit internal forces and deformations in structural elements when extreme events occur. This positive aspect is very interesting when the dimensions of the structure are large. Herein, an updated numerical model of an existing suspension bridge is developed in a commercial finite element work frame, starting from original data. This model is used to reevaluate an optimization procedure for a passive control strategy, already proven effective with a simplified model of the buffeting wind forces. Such optimization procedure, previously implemented with a quasi-steady model of the buffeting excitation, is here reevaluated adopting a more refined version of the wind-structure interaction forces in which wind actions are applied on the towers and the cables considering drag forces only. For the deck a more refined formulation, based on the use of indicial functions, is adopted to reflect coupling with the bridge orientation and motion. It is shown that there is no variation of the previously identified optimal passive configuration.

**Keywords:** suspension bridge; optimal control; drag forces; dynamic interaction; design

## 1. Introduction

Long span and limited response under several different dynamic conditions are general requirements for modern suspension bridges design. An important contribution to the solution of this difficult task can be given by the Structural Control discipline.

Pursuing this goal, the authors have in the past studied the feasibility of controlling wind induced vibration in long span suspension bridges through passive and semi-active control systems (Domaneschi and Martinelli 2009, 2011, 2013). These studies were based on a model of an existing suspension bridge, developed at the numerical level inside the ANSYS finite element (FE) framework. The wind loading was considered the main dynamic excitation, through drag forces applied on the towers, the cables and the deck of the suspension bridge in the framework of the quasi-steady theory.

*Corresponding author, Ph.D. Contract Professor, E-mail: marco.domaneschi@polimi.it
[a] Ph.D. Assistant Professor, E-mail: luca.martinelli@polimi.it


http://www.techno-press.org/?journal=was&subpage=8 ISSN: 1226-6116 (Print), 1598-6225 (Online)

a specific wind intensity, was studied at different levels of wind intensity to make the results general.

The attention was initially focused on passive control systems, also known as self-defense ones, since they allow for dissipating energy and change the structural stiffness without using external active power. Also, they have the advantage of being robust, working independently from one another, and more stable than the active systems, by not injecting external power into the structural system. They are easier to implement, and enjoy lower operating and maintenance costs also.

Such control strategies require the use of properly positioned structural elements, able to dissipate the energy fed into the structure by dynamic actions and to decouple the superstructure motion from the supports. Their main disadvantage is not to be able to adapt themselves to different levels of the dynamic loads. For this reason, semi-active control strategies were later also studied by the authors in an original decentralized configuration on the suspension bridge model. These semi-active strategies adopted as a starting point, the operating parameters for the devices associated to the passive control configuration previously identified as optimal.

The response of suspension bridges to wind excitation is a problem of wide concern in literature and several studies on wind loading simulation through indicial functions have also been proposed.

Salvatori and Spinelli (2006) recently studied a suspension bridge response to wind excitation by means of FE numerical simulations and Monte Carlo method on a simplified structural model. Self-excited effects are included through the indicial function formulation and the buffeting is considered according to the quasi-steady model. They observed the role of nonlinearities in deemphasizing the presence of a critical flutter wind velocity and also an underestimation of the structural response by a fully correlated flow.

Chen and Kareem (2001) report on a time domain approach for predicting the buffeting and flutter responses with aerodynamic nonlinearities through static force coefficients and flutter derivatives. A slightly higher response, than the conventional linear analysis, is pointed out for the analysis involving the aerodynamic nonlinearity. A subsequent investigation by the same authors (Chen and Kareem 2003) investigates the effects of low-frequency components of turbulence on flutter and buffeting response for long span suspension bridges. Aerodynamic characteristics, sensitive to the angle of incidence, have been presented demonstrating their significance for accurately predicting the aeroelastic response, with respect to the static angle of attack of the bridge deck.

Ubertini (2011) analyzed the aeroelastic stability of bridge decks by means of self-excited loads with the aid of aerodynamic indicial functions approximated by truncated series of exponential filters. The investigation is focused in particular on the implementation of tuned mass dampers for improving the bridge stability with particular care to multiple application of such devices.

In this paper the optimization process for passive control systems, previously applied within a simplified model of the buffeting excitation comprising only the drag forces, is reevaluated in association with a more refined description the wind-structure interaction forces. This refined description in time domain is based on modeling the drag force as completely non linear, within the quasi-steady theory, while adopting for the lift force and the aerodynamic moment a linearized form with corrections for frequency dependent loading using indicial functions (Scanlan *et al*. 1974, Salvatori and Borri 2007). Finally, the field of turbulent wind velocities has been simulated as a spatially correlated process according to a literature model (Solari and Piccardo 2001).

## 2. Geometry and numerical model

The suspension bridge model in this work is inspired by the Shimotsui-Seto Bridge, in Japan, spanning from the side of Mt. Washu to the Hitsuishijima Island. The length of the bridge is 1400 m with a main span of 940 m. The towers are 149 m tall, while the vertical distance of the main girder from the towers foundation has been assumed at 31 m. Fig. 1(a) shows the main dimensions of the bridge, Fig. 1(b) depicts a general overview of the stiffened truss type steel deck. The main cables, the hangers and the main girder are in steel, the towers are assumed as built in concrete (Romano 2009).

Two numerical models of the suspension bridge have been developed in the ANSYS framework at different refinement levels. A first, more detailed, model (Fig. 2(a)), implements an almost complete correspondence between structural and FE elements. Its geometrical and mechanical properties have been assessed by the match of the first four natural periods and modal shapes with those measured on the real structure. The purpose of this model was to aid in the development of a second, simpler, one (Fig. 2(b)). This last has been derived to perform numerically non linear transient analyses under wind loading.

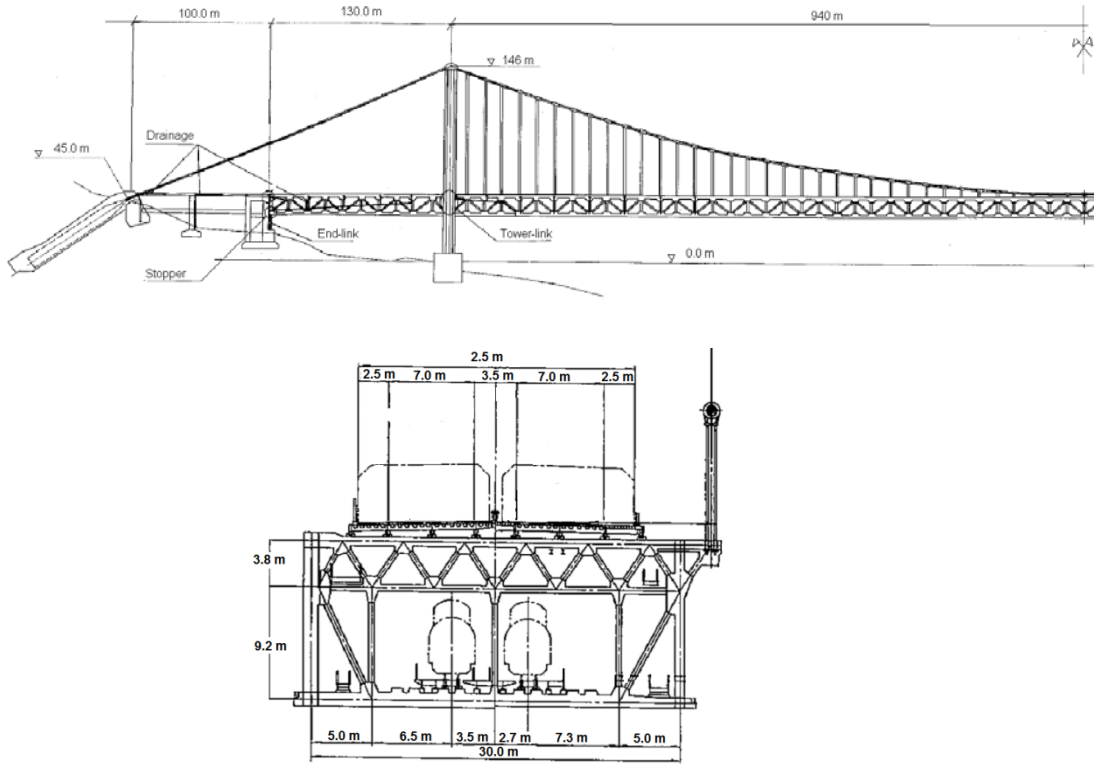


Fig.1 (a) Bridge geometry and (b) Detail of deck transversal section. Courtesy of Mr. M. Nishitani HBSE-JP

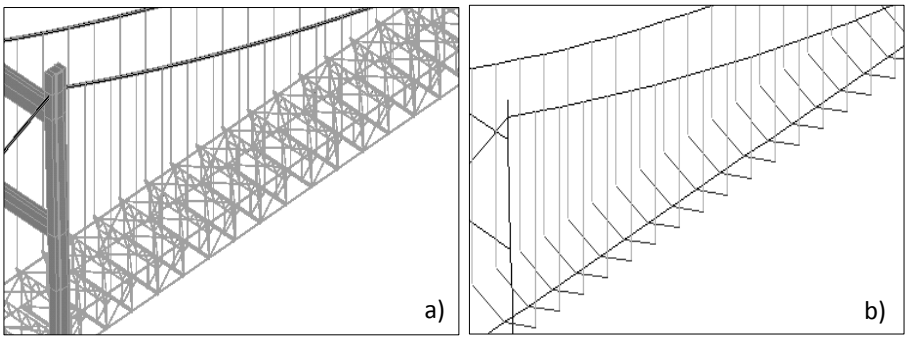


(a) One to one representation (b) Equivalent beam

Fig. 2 Main girder FE details: complete (a) and simplified (b) version

Table 1 Modal frequencies for the real (Courtesy of Mr. M. Nishitani HBSE-JP) and the simplified bridge model

| *Mode* | *Measured on the structure [Hz]* | *From the detailed model [Hz]* | *From the simplified model [Hz]* | *Modal shape* |
|---|---|---|---|---|
| 1 | 0.104 | 0.099 | 0.089 | Lateral symmetric |
| 2 | 0.157 | 0.149 | 0.160 | Vertical anti-symmetric |
| 3 | 0.196 | 0.235 | 0.219 | Vertical symmetric |
| 4 | 0.255 | 0.255 | 0.260 | Lateral anti-symmetric |

Table 2 Modal frequencies of the simplified bridge model

| *Mode* | *Modal shape* | *#* | *Frequency [Hz]* |
|---|---|---|---|
| L1 | Lateral symmetric | 1 | 0.089 |
| L2 | Lateral anti-symmetric | 8 | 0.260 |
| L3 | Lateral symmetric | 14 | 0.405 |
| L4 | Lateral anti-symmetric | 27 | 0.696 |
| L5 | Lateral symmetric | 33 | 0.862 |
| T1 | Torsional symmetric | 14 | 0.405 |
| T2 | Torsional anti-symmetric | 23 | 0.582 |
| T3 | Torsional symmetric | 33 | 0.862 |
| V1 | Vertical anti-symmetric | 2 | 0.160 |
| V2 | Vertical symmetric | 6 | 0.219 |
| V3 | Vertical symmetric | 9 | 0.321 |
| V4 | Vertical anti-symmetric | 15 | 0.436 |
| V5 | Vertical symmetric | 25 | 0.630 |
| V6 | Vertical anti-symmetric | 32 | 0.844 |

The accuracy of this simpler model was assessed by comparing its first modal frequencies, listed in Table 1, both against the experimental values of the same and those coming from the detail bridge model, while the higher modes were assessed against the results derived from the

detail bridge model only, since no experimental data was available. Modal shapes were validated by application (Allemang and Brown 1982) of the Modal Assurance Criterion (MAC). The frequencies of the higher modes are listed in Table 2. Intermediate modes not listed in Table 2 involve mainly the main cables and the suspenders. The interested reader is pointed to (Domaneschi and Martinelli 2013, Romano 2009) for further details on the numerical models.

In the following, the model will be referred to a system of global axis in which axis $X$ is normal to the bridge span, axis $Y$ is vertical while axis $Z$ is along the bridge span. The aerodynamic forces and the turbulence, will instead be described with reference to the components parallel to an along-wind axis $x$, a cross-wind axis $y$ and a vertical axis $z$, respectively.

## 3. Aerodynamics forces and wind field

In previous works by the authors (Domaneschi and Martinelli 2009, 2011, 2013) a control strategy has been proposed, and proven effective, for wind loading in conjunction with a simplified model of the buffeting wind forces which included, in the framework of the quasi-steady theory, the drag forces only. In this work a reevaluation of the control strategy is carried out adopting a more refined representation of the fluid interaction forces to assess if the one originally used was adequate.

In the quasi-steady theory the drag force $D_0$, the lift force $L_0$ and the aerodynamic moment $M_0$ are expressed as a non-linear function of the attack angle $\alpha$ as

$$\begin{cases} D_0 = \frac{1}{2}\rho U^2 B C_D(\alpha) \\ L_0 = \frac{1}{2}\rho U^2 B C_L(\alpha) \\ M_0 = \frac{1}{2}\rho U^2 B^2 C_M(\alpha) \end{cases} \tag{1}$$

The angle of attack $\alpha$ is the angle between the relative wind velocity $V_r$ with respect a reference direction on the bridge cross-section (here, the horizontal direction in the equilibrium configuration under gravitational loads). The aerodynamic coefficients $C_D$, $C_L$ and $C_M$ are measured in the wind-tunnel in steady conditions.

The lift force $L$ (normal to $V_r$) and drag force $D$ (along $V_r$) in the cross-section reference are related to the forces in the global reference system by a transformation involving a projection (e.g., Martinelli and Perotti 2001).

In this work the drag force $D(\alpha)$ is modeled as completely non linear, within the quasi-steady theory (see $D_0$ in Eq. (1)). The lift force $L(\alpha)$ and the aerodynamic moment $M(\alpha)$ are expressed in time domain in a linearized form starting from the quasi-steady equations (Stoyanoff 2001), with added correction coefficients for frequency dependent loading using the indicial functions approach (Scanlan *et al*. 1974, Salvatori and Borri 2007).

### *3.1 Indicial functions approach*

For the sake of simplicity we initially consider the lift force only; a similar approach and results can be applied to the aerodynamic moment as well. From the quasi-steady theory, the lift force $L(\alpha)$ is a function of the angle of attack $\alpha$

$$L(\alpha) = \frac{1}{2}\rho U^2 B C_L(\alpha) \tag{2}$$

It can be shown that it is often possible within a limited range of variation for $\alpha$ (e.g. -5°,+5°) to assume the derivatives of the aerodynamic force coefficients as constants. Exploiting this, with a Mc Laurin expansion of $C_L$ around $\alpha = 0$, we have

$$L(\alpha) = \frac{1}{2}\rho U^2 B (C_L(0) + C_L'\alpha) \tag{3}$$

In general, a sudden (step) change in $\alpha$ at time $t = 0$ (here denoted as $\alpha_0$) will produce its full effect only after some time is elapsed since the flux around the body needs some time to stabilize again. In 1925 Wagner showed that the lift can also in this case be considered as a liner function of $\alpha$ , and gave for the thin airfoil case the theoretical expression for the indicial growth function $\varphi(s)$ of the lift as a function of a non dimensional time $s=2Ut/B$, where $U$ is the average velocity of the stream and $B$ the chord length of the airfoil

$$L(s) = \frac{1}{2}\rho U^2 B C_L' \alpha_0 \varphi(s) \tag{4}$$

The indicial function describes the evolution in time of the lift force induced by a step change of the angle of attack. A similar function can be defined for a step change of the vertical velocity $\dot{z}$ of the cross-section. We will initially consider only a change of $\alpha$.

Linearity of $L$ in $\alpha$ in Eq. (3) allows to obtain the lift force at time $s$ as a convolution of the increments of $\alpha$

$$L(s) = \frac{1}{2}\rho U^2 B C_L' \int_{-\infty}^{s} \varphi(s-\sigma)\alpha'(\sigma)d\sigma \tag{5}$$

Which, assuming $\sigma_1 = s - \sigma$, can be recast as

$$L(s) = \frac{1}{2}\rho U^2 B C_L' \left[ \varphi(0)\alpha(s) + \int_0^{\infty} \varphi'(\sigma_1)\alpha(s-\sigma_1)d\sigma_1 \right] \tag{6}$$

In 1974 Scanlan et al. proposed a similar form for the aerodynamic forces of non-streamlined bodies

$$D(s) = qBC'_D [\Phi_{D\alpha}(0)\alpha(s) + \Phi_{Dz}(0)\frac{\dot{z}(s)}{U} + \Phi_{Dx}(0)\frac{\dot{x}(s)}{U} + \int_{-\infty}^{s} \Phi'_{D\alpha}(s-\mu)\alpha(\mu)d\mu + \tag{7}$$
$$+ \int_{-\infty}^{s} \Phi'_{Dz}(s-\mu)\frac{\dot{z}(\mu)}{U}d\mu + \int_{-\infty}^{s} \Phi'_{Dx}(s-\mu)\frac{\dot{x}(\mu)}{U}d\mu]$$

$$L(s) = qBC'_L [\Phi_{L\alpha}(0)\alpha(s) + \Phi_{Lz}(0)\frac{\dot{z}(s)}{U} + \tag{8}$$
$$+ \Phi_{Lx}(0)\frac{\dot{x}(s)}{U} + \int_{-\infty}^{s} \Phi'_{L\alpha}(s-\sigma)\alpha(\sigma)d\sigma + \int_{-\infty}^{s} \Phi'_{Lz}(s-\sigma)\frac{\dot{z}(\sigma)}{U}d\sigma + \int_{-\infty}^{s} \Phi'_{Lx}(s-\sigma)\frac{\dot{x}(\sigma)}{U}d\sigma]$$

$$M(s) = qB^2C'_M [\Phi_{M\alpha}(0)\alpha(s) + \Phi_{Mz}(0)\frac{\dot{z}(s)}{U} + \Phi_{Mx}(0)\frac{\dot{x}(s)}{U} + \int_{-\infty}^{s} \Phi'_{M\alpha}(s-\tau)\alpha(\tau)d\tau + \tag{9}$$
$$+ \int_{-\infty}^{s} \Phi'_{Mz}(s-\tau)\frac{\dot{z}(\tau)}{U}d\tau + \int_{-\infty}^{s} \Phi'_{Mx}(s-\tau)\frac{\dot{x}(\tau)}{U}d\tau]$$

Where $\Phi_i$ are the equivalent of $\varphi$ for the buff body and $q = ½\rho U^2$ is the dynamic pressure. Eqs.

(8) and (9) will be followed herein to express the lift force and the aerodynamic moment; the last with respect to the centroid of the bridge cross-section. The different behavior of $\varphi$ and $\Phi$ can be appreciated in Fig. 3 (redrawn from Scanlan *et al*. 1974). In this picture it is emphasized as the indicial functions are asymptotic to 1 and, for a buff body, can become initially larger than 1.

Normally, the functions $\Phi_i(s)$ are approximated by one or more exponential groups of the type

$$\Phi_i = a_{0,i} - a_{1,i}e^{(-b_{1,i}s)} - a_{2,i}e^{(-b_{2,i}s)} \tag{10}$$

which depend on five constants each. The coefficients $a_{0,i}$, $a_{1,i}$, $b_{1,i}$, $a_{2,i}$ $b_{2,i}$ are estimated by minimizing the differences in case of a harmonic variation of $\alpha$, $x$, $y$ between the aerodynamic forces computed in time domain using Eqs. (7) and (9), with $\Phi$ as in Eq. (10), and the same forces computed in frequency domain using the so called "flutter derivatives", which are experimentally extracted from measurement (normally in a wind tunnel) of a sectional model of the bridge cross-section.

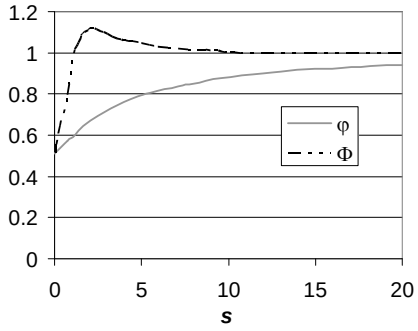


Fig. 3 Indicial function $\varphi$ by Wagner and indicial function $\Phi$ for a bridge deck; redrawn from (Scanlan *et al*. 1974)

In using Eqs. (7) and (9) a practical problem arises in that the aerodynamic forces have to be computed with a convolution integral starting from -∞. Due to $\varphi(s)$ or $\Phi_i(s)$ rapidly converging to 1, the system is rapidly loosing memory of previous variations of $\alpha$, that can then be readily included in the first term in parenthesis in Eq. (3). The convolution integral can then be computed only on the past interval of the order of 10 units of non-dimensional time (Borri and Hoeffer 2000). Furthermore, whenever a representation through exponential groups is adopted the convolution integral from -∞ to the present time can be further simplified, see (Leishman 2000).

Since the flutter derivatives for the Shimotsui Seto Bridge were not available in literature, in this work the coefficients of the exponential groups identified from the flutter derivatives of the Akashi Kaikyo bridge have been adopted. This bridge has a girder section which is geometrically similar to that of the bridge under study (see Fig. 1(b) and Kitagawa 2004) although it presents a slot and a stabilizer in the center of the truss girder that are not present in the Shimosui Seto bridge cross-section.

Finally, it is worth remembering that the coefficient $a_{0,i}$ in Eq. (10) must be set equal to one in all considered indicial functions to make consistent this approach, when $s$ is very large, with the quasi-steady theory results (Zhang *et al*. 2011). The remaining coefficients for the lift force and the aerodynamic moment are as reported in (Caracoglia and Jones 2003) for a step change of the attack angle $\alpha$ or of the vertical velocity $\dot{z}$ of the bridge cross-section, and are listed in Table 3.

Table 3 Coefficients of the Indicial Functions

| *Function* | $a_1$ | $b_1$ | $a_2$ | $b_2$ |
|---|---|---|---|---|
| $\Phi_{Lz}$ | -0.365 | 0.021 | -11.652 | 7.235 |
| $\Phi_{L\alpha}$ | -0.392 | 0.008 | -3.653 | 1.155 |
| $\Phi_{Mz}$ | 0.039 | 0.000 | 0.000 | 0.000 |
| $\Phi_{M\alpha}$ | 0.073 | 0.025 | 1.758 | 7.098 |

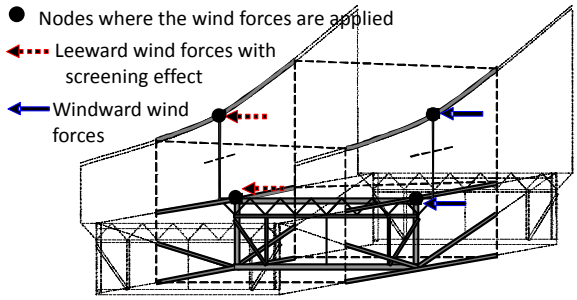


Fig. 4 Scheme of wind forces application on the deck and main cables

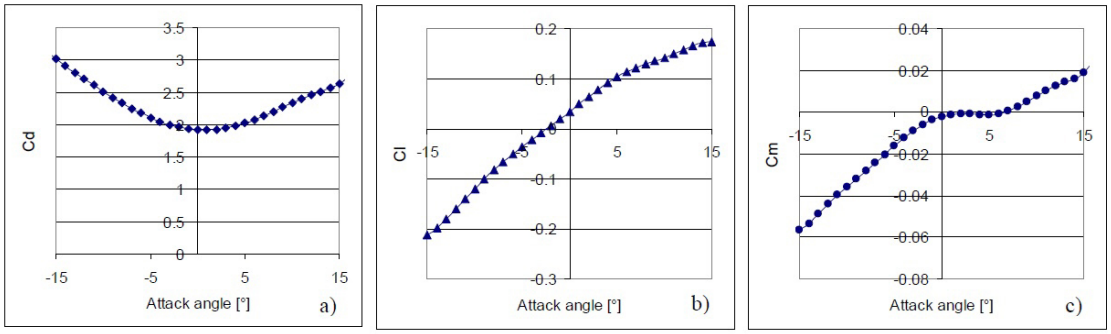


(a) (b) (c)

Fig. 5 Wind tunnel test curves of the bridge deck: drag (a), lift (b) and moment (c) coefficients as function of attack angle. Courtesy of Mr. M. Nishitani HBSE-JP

### *3.2 Drag forces*

The external wind load is applied to the towers, the deck and the cables in the horizontal direction, transversal to bridge span (Fig. 4). The contribution of only the drag forces is accounted for according to Eq. (1) for the towers and the cables. For the deck the drag force is computed from the quasi-steady theory with Eq. (1) while the lift force and the moment are computed with the indicial function formulation of Eqs. (8) and (9). Drag force on the suspenders is split into two parts applied respectively to the main cable (top) and to the main girder (bottom), see Fig. 4.

The values of the drag coefficients for the towers, the hangers and the main cables are evaluated from literature (ESDU 81027 1988, ESDU 71012 1971, CNR-DT 207 2008), taking into account the screening effect of the windward elements. Evaluation of the coefficients for the deck is performed from the original wind tunnel test curves as depicted in Fig. 5. In particular, the relation between the attack angle and the bridge deck drag coefficient is shown in Fig. 5(a).

The adopted values of drag coefficients are listed in Table 4. From these, the drag forces are computed and applied at the nodes of the numerical model by knowledge of the tributary areas of the nodes and the wind velocities at the same.

Table 4 Drag coefficients

| | $C_D$ | *Screening effects* |
|---|---|---|
| *Deck* | Wind tunnel tests (Fig. 5) | - |
| *Suspenders* | 0.65 | - |
| *Main cables* | 0.7 | Considered |
| *Towers* | 1.84 | Considered |

### *3.3 Simulation of the wind field*

To compare the results of this study to those of the previous ones (Domaneschi and Martinelli 2009, 2011, 2013) the reevaluation of the control strategy design is performed assuming the structural model is subjected to the same turbulent wind field that was used previously. The mean velocity is transversal to the longitudinal bridge axis and a mean wind velocity of 45.8 m/s has been considered in the required transient dynamic analyses.

The wind velocity field is simulated as a 3D spatially correlated process, non-homogeneous in space to consider the atmospheric boundary layer. The turbulent velocities are computed at the initial position of each node of the FE model in the generated 3D turbulent wind field.

Turbulence is modeled by generating artificial velocity time-histories, according to the 3D turbulence model by Solari and Piccardo (2001). This model is based on the definition of direct spectral densities and coherency functions. The latter can relate different components at the same points (‘point’ coherencies) or equal components at different points (‘space’ coherencies). Decay of space coherencies with distance is of exponential type. The model is completely defined when the average velocity, the terrain factor, the roughness length and the minimum height are given, here by assuming the values in Eurocode 1 (2005) for sea or coastal areas (terrain category 0).

In this turbulence model, the component $\varepsilon = u, v, w$ in the along-wind axis $x$, the cross-wind axis $y$ and the vertical axis $z$, respectively, of the turbulence at a point at height $z$ above the ground is defined in the frequency domain by its Power Spectral Density (PSD) function as

$$S_\varepsilon(z,f) = \sigma_\varepsilon^2 \frac{d_\varepsilon L_\varepsilon(z)/\overline{u}(z)}{\left[1+1.5 d_\varepsilon f L_\varepsilon(z)/\overline{u}(z)\right]^{5/3}} \tag{11}$$

where $\sigma_\varepsilon^2$ is the variance of the turbulent component $\varepsilon$, $L_\varepsilon$ is the integral length scale for that component and $d_\varepsilon$ is a coefficient (having value: $d_u = 6.868$, $d_v = d_w = 9.434$) and $f$ is the frequency.

The model relates two different components, $\varepsilon$ and $\eta$, of the turbulence acting at two different

point in space, $M_k$ and $M_l$, by the cross-Power Spectral Density function

$$S_{\varepsilon\eta,kl} = \sqrt{S_{\varepsilon\varepsilon} \cdot S_{\eta\eta}} \cdot \mathrm{coh}_{\varepsilon\eta,kl}\left(M_k, M_l, f\right) \tag{12}$$

where $\mathrm{coh}_{\varepsilon\eta,kl}\left(M_k, M_l, f\right) = \mathrm{sgn}\left(\Gamma_{\varepsilon\eta}\right)\sqrt{\Gamma_{\varepsilon\eta}\left(z_k, f\right)\cdot\Gamma_{\varepsilon\eta}\left(z_l, f\right)}\cdot\sqrt{\Lambda_{\varepsilon}\left(M_k, M_l, f\right)\cdot\Lambda_{\eta}\left(M_k, M_l, f\right)}$.

is the coherency function that depends on the point coherence $\Gamma_{\varepsilon\eta}(z,f)$ and on the spatial coherence $\Lambda_{\varepsilon}(M_k, M_l, f)$. Only the along wind component and the vertical one are assumed correlated, hence $\Gamma_{uv} = \Gamma_{vw} = 0$.

The wind velocity records are generated, according to the procedure by Hao *et al*. (1989), in series of $n_{st}$ points starting from the time history at a starting node. Based on the analysis of the preliminary results for a limited number of cases, the along-wind component only has been retained in completing all the subsequent analyses of this study.

The velocity time histories $u_i$ at the nodes in the numerical model are obtained by the finite series

$$u_i\,(M_i, t) = \sum_{m=1}^{i}\sum_{n=1}^{N} A_{im}\left(\overline{\omega}_n\right)\cos\left[\overline{\omega}_n t + \beta_{im}\left(\overline{\omega}_n\right) + \phi_{mn}\right] \qquad i = 1...n_{st} \tag{13}$$

where the circular frequencies are assumed varying in the interval $-\omega_N \le \omega \le \omega_N$, $\omega_N$ is the Nyquist frequency, $\phi_{mn}$ are the phase angles, described as random variables with uniform probability density between 0 and $2\pi$ which are statistically independent from $\phi_{rs}$ for $m \ne r$ and $n \ne s$. The amplitudes $A_{im}$ and the phase angles $\beta_{im}$ are selected so as to satisfy Eqs. (11) and (12).

## 4. Reevaluation of the optimal passive control system

In previous works by the authors (Domaneschi and Martinelli 2009, 2011, 2013) a control strategy has been proposed, and proven effective, for wind loading. The strategy comprised finding the optimal parameters for the hysteretic devices of a passive control system, in conjunction with a model of the buffeting wind forces based on the quasi-steady theory. Here, a reevaluation of the optimization procedure and the performance of the control strategy is carried out adopting the more refined representation of the fluid interaction forces, previously described, to assess if the simpler description, originally used, was satisfactory.

When designing the additional hysteretic damping for a structure, the number, the size and the location of the dissipative devices should be decided in order to achieve a desirable response level. Any procedure developed for sizing and placing the control devices should be characterized by simplicity, efficiency and practicality (Garcia and Soong 2002, Zhang and Soong 1992). It follows that any algorithm for the devices optimization should require analytical techniques normally in use by design engineers (simplicity), minimizing the amount of devices (efficiency) and the number of different damper sizes (practicality).

The buffeting, low frequency, vibrations passive control on the Shimotsui-Seto Bridge is performed in (Domaneschi and Martinelli 2013) by the application of a methodology inspired by the *Sequential Placement Algorithm* (Zhang and Soong 1992). The identification of the optimal system requires the definition of objective functions, the position of the control elements and the identification of the devices optimal parameters.

The whole optimization procedure is characterized by means of :

- *variables*, represented by devices positions and damping,
- *restraints*, consisting in the lowest number of different devices,
- *targets*, the optimal damping values for the control dampers (relative minimum point of the objective functions).

The control system designed following the proposed optimization methodology presents also limitations: one wind velocity is exclusively selected, so, for different wind intensities, the passive system protection cannot be the optimal one. However, as the control theory postulates, this limit characterizes all passive control systems for structural applications (Domaneschi 2010, 2012).

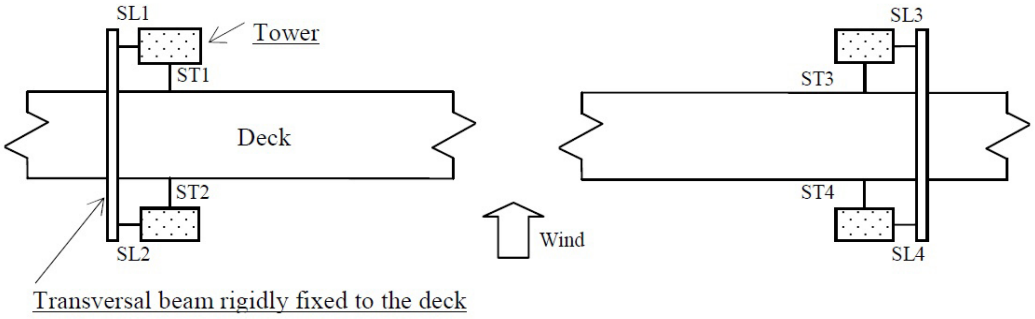


Fig. 6 Devices positioning on the bridge deck, top view

The natural choice for placement of the devices was to set them at the deck-tower connection points, characterized by the higher stiffness of the towers in comparison to the main girder of the bridge. Those positions are directly next to the maximum deck displacements sites at the mid-span.

The inclination of the dampers with respect to the longitudinal axis of the bridge has been specifically considered as an additional variable through the use of two classes of dampers, transversal deck dampers, denoted by ST, and longitudinal deck dampers, indicated with SL as shown in Fig. 6. For the last type, two deck stiffening beams need to be introduced with the task of creating a support for the insertion of the longitudinal dampers.

Dampers ST give the largest contribution to the control of the system while dampers SL play a secondary role in which they create a dissipative torque which reduces part of the transverse displacements due to the rotation of the deck around the vertical axis at the towers. Two device typology results from the general symmetry which characterizes the structural scheme of the Shimotsui-Seto suspension bridge.

Therefore, the optimization procedure for the passive control system of the Shimotsui-Seto bridge can be summarized in the following steps:

1. find the positions where to place transversal (ST) and longitudinal (SL) devices;
2. consider only the SL devices and find the parameters that maximize the structural damping;
3. consider the SL devices with the configuration fixed by step 2 and find the parameters of the ST devices that minimize the objective functions.

The performances and the effectiveness of this control design can be found in (Domaneschi and Martinelli 2009, 2011, 2013) for the case of wind interaction forces limited to drag forces

described within the quasi-steady theory and devices simulated by the Bouc-Wen model (Wen 1976).

After presenting the model of the control devices, in the following we will next summarize the choice of the objective functions and the reevaluation of the control strategy within the refined description of the wind forces.

### 4.1 Model of control devices

The numerical simulation of control devices allows for the evaluation of their efficiency into complicated structural systems under stochastic external forces. Among the others, the Bouc-Wen model (Wen 1976) has been often selected for the simulation of dissipative passive and semi-active devices (Domaneschi 2010, 2012), such as metallic dampers, rubber bearings, piezoelectric dampers (Low and Guo 1995), magneto-rheological dampers (Spencer *et al*. 1997) and electro-inductive devices (Casciati and Domaneschi 2007).

The choice we made to idealize passive and semi-active devices by the Bouc-Wen law is supported by the physical and mathematical consistency of this model (Erlicher and Point 2004) and the excellent correspondence between the experimental and numerical results. More recently, the dynamic stability of the model has been investigated in (Ikhouane *et al*. 2007a), where the domain limits for the model parameters are fixed, while the model passivity, among other general properties, is established in (Ismail *et al*. 2009). In light of these considerations, the Bouc-Wen model has been adopted for simulating control devices on the suspension bridge model and their optimization procedure.

According to the Bouc-Wen endochronic hysteretic model, the equations governing the restoring force produced in each passive devices are given as

$$\dot{z}_h = A\dot{x}_r - \beta\dot{x}_r|z_h|^n - \gamma|\dot{x}_r|z_h|z_h|^{n-1} \tag{14}$$

$$\Phi(x_r,t) = (1-\alpha)kz_h + \alpha k x_r + c\dot{x}_r \tag{15}$$

where $x_r$ is the relative displacement between the device ends, $\dot{x}_r$ the relative velocity, $z_h$ is an auxiliary variable allowing one to introduce a smooth hysteretic behaviour, $k$ the pre-yielding stiffness, $\alpha$ the ratio between post and pre-yielding stiffness ($\alpha=1$ provides an elastic response and $\alpha=0$ an elastic-perfectly-plastic behaviour) and $A, \beta, \gamma, n$ are time invariant parameters defining the amplitude and the shape of the cycles, the linearity in unloading and the smoothness of the transition from the pre- to the post-yield region. In particular, $A$ is related to the initial stiffness, $\beta$ regulates the cycle amplitude and consequently the dissipation level ($\beta\rightarrow 0$ for low energy dissipation), $\gamma$ defines the unloading path in the hysteresis, $n$ the smoothness of the transition. The relationship between the parameters that appear in the differential Eq. (14) and the shape of the obtained hysteresis loops is deepen in (Ikhouane *et al*. 2007b), using a normalized form of the model.

Variable $\Phi(x_r,t)$ in Eq. (15) is the control force (axial) provided by the device at its ends. The problem related to the model identification can be solved by considering the physical meaning of the parameters: in particular the axial yielding force $\Phi_y$, for value $A = 1$ and $\alpha$ close to zero, descends from some algebra and assumes the following form

$$\Phi_y = \frac{k}{(\beta+\gamma)^{1/n}} \tag{16}$$

For the identification procedure of the Bouc-Wen model, the interested reader is pointed to (Domaneschi 2012).

To carry out the computations required by this work, the constitutive law given by the Bouc-Wen model has been implemented into the commercial ANSYS FE framework by an external user element. It consists in a Fortran executable called, at each step of analysis, by the script governing the ANSYS analysis. The procedure is carried out writing special routines in the ANSYS parametric language (APDL), capable of extracting the kinematics of the nodal points joined by Bouc-Wen elements, write appropriate interface files, call the external executable, read and then apply to the structural model the externally computed control forces. In particular, the process of calling the external executable from the main script was carried out using the ANSYS command "/SYS". More details on the Bouc-Wen model implementation in ANSYS can be found in (Domaneschi and Martinelli 2012, Domaneschi *et al*. 2010).

The damping provided to the whole bridge system by the control devices is evaluated at each stage of the optimization procedure by tuning the model parameters. Particularly, fixed the device pre-yielding stiffness $k$, the axial yielding force $\Phi_y$ (Eq. (16)) is tuned by changing parameters $\beta$ and $\gamma$, while the remaining ones are kept fixed ($\alpha = 0.02$, $n = 1$ and $A = 1$).

The Bouc-Wen parameters, selected by the abovementioned procedure, reproduce the hysteresis signature coming from an innovative electro-inductive device characterized in laboratory for structural control applications on long span bridges (Casciati and Domaneschi 2007). It represents a fascinating solution for the feasibility of larger passive devices of this type to be installed in long span bridges. This is of interest due to two facts: that they are much shorter than passive hydraulic dampers of identical maximum stroke and that they can easily be converted into the semi-active type, adapting themselves to different seismic intensity levels (Domaneschi 2010, Domaneschi and Martinelli 2012) by using specific control laws (Domaneschi 2012). An additional aspect to underline is the self-centering ability after an extreme loading event, realigning the deck with its original axis and the towers.

In this light, the presented results are also intended as a realistic validation of such innovative damper implementation on a suspension bridge by using accurate models of the structure, the devices and the wind loading conditions.

### *4.2. Objective functions and results*

Standard deviation is a valuable parameter for directly identifying peak values of structural variables, such as internal forces and displacements, and indirectly also for a statistical estimation of the peak value of a variable.

In this light, the objective functions from the adopted optimization procedure, were fixed as the standard deviation of the internal forces at the base of the towers and of the transverse mid-deck displacement: identified respectively as the shear $T_x$, the bending moment $M_z$ and the displacement $U_x$ in the global frame of reference (Domaneschi and Martinelli 2013). These functions are minimized by varying the damping contribute, due to the passive control system implementation, through a change of the variables that govern the control devices constitutive law.

The optimization procedure was carried out considering a single excitation having a mean wind speed $U_m = 45.8$ m/s according to the following steps:

1. evaluation of the optimal parameters for the longitudinal devices SL that maximize their contributes to the structural damping;

2. investigation of the optimal characteristics for the transversal dampers ST when the SL devices have parameters coming from step 1.

Step 1 was carried out considering the bridge controlled only by the contribution of the SL devices. Step 2 consists in the identification of the damping characteristics that minimize the objective function, by varying the parameter $\Phi_y$ of the ST devices.

The optimal configuration of the whole passive control system was identified in (Domaneschi and Martinelli 2013), considering the quasi-steady model of the buffeting forces, by the Bouc-Wen parameters: $A = 1$, $n = 1$, $\alpha = 0.02$, $\beta = \gamma = 330$, $k = 40000$ kN/m, $\Phi_y = 60$ kN for the SL devices; $A = 1$, $n = 1$, $\alpha = 0.02$, $\beta = \gamma = 250$, $k = 150000$ kN/m, $\Phi_y = 300$ kN for the ST devices (Domaneschi and Martinelli 2013).

This process is herein carried out for the bridge structure with the refined model of the wind interaction forces described in the Section 3. The results are compared in Figs. 7-9 to the original ones from (Domaneschi and Martinelli 2013), obtained using a much simpler model of wind interaction forces. Such figures describe the variation of the standard deviation (Figs. 7(a)-9(a)) and of the mean values (Figs. 7(b)-9(b)), respectively for $T_x$, $M_z$ and $U_x$, as functions of yield force $\Phi_y$ and stiffness $k$ of the ST devices. From these results we have, on the one hand, that the standard deviation of the transverse displacement $U_X$ (Fig. 9(a)) upholds, reaching its minimum at a value of the ST dampers elastic limit $\Phi_y = 300$ kN, while the standard deviations of the internal forces (Figs. 7(a)-8(a)) still reach their minima at $\Phi_y = 200$ kN.

This is in accord with the concept of Pareto (Pareto 1927) optimal points, that the values taking to the minimum of an objective function do not imply necessarily that the remaining ones do attain their minima as well. On the other hand, the mean values (Figs. 7(b)-9(b)) change, albeit only slightly, showing less severe values for the tower base shear force and bending moment when the wind loading forces are computed through the quasi-steady approach.

In light of the results from Figs. 7-9, a fist outcome is obtained: the optimal passive control parameters coming from use of the quasi-steady model of the buffeting loading rest confirmed also when reevaluated by adopting a more refined version of the fluid interaction forces.

Furthermore, it has to be noted as the standard deviation of the internal forces at the base of the towers and the deck mid-span displacement (Figs. 7(a)-9(a)), are always lower than those obtained with the simplified approach, consistently with the results in (Chen *et al*. 2000). This is additionally confirmed by looking at Table 5, which compares the results in terms of mean, standard deviation and maximum intensity values, for the optimal passive control systems, between the two considered approaches to buffeting forces. In addition to $T_X$, $M_Z$ at the towers base, and $U_X$ at the mid-span, the deck bending moment $M_Y$ around the vertical axis has also been listed at the mid-span and quarter-span of the deck. The simplified approach shows higher maximum and standard deviation values for all reported structural variables.

These results, which consider the additional internal force $M_Y$, with respect to the objective functions, confirm how the simplified wind loading model can lead to an overestimation of the structural response. The consequence is that this simpler wind loading model can be used to design solution that will have a good chance to be satisfactory also when the refined model will be used.

Fig. 10 depicts the comparison, in the frequency domain, of the two considered approaches to buffeting forces in terms of base tower shear force $T_X$ (Fig. 10(a)), base tower bending moment $M_Z$ (Fig. 10(b)), mid-span displacement $U_X$ (Fig. 10(c)), quarter-span bending moment $M_Y$ (Fig. 10(d)).

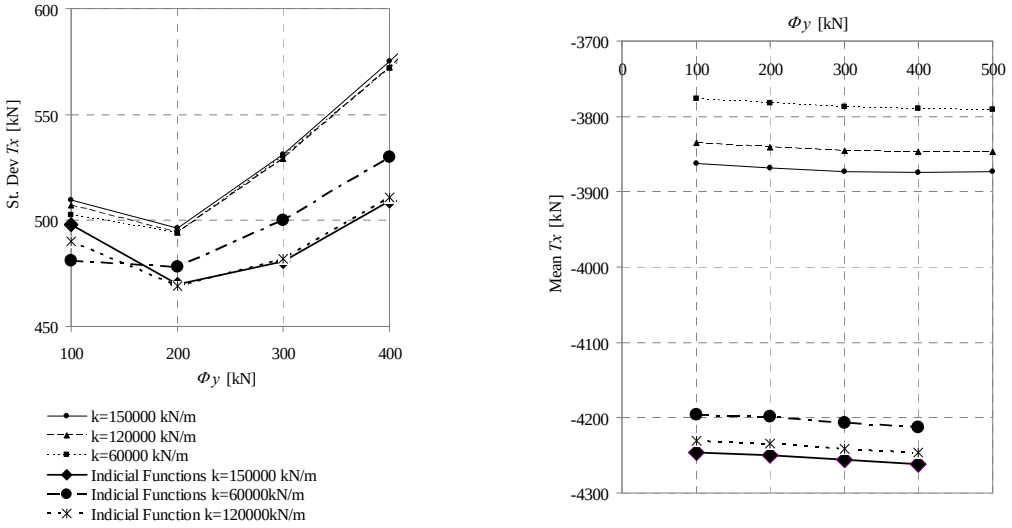


Fig. 7 Standard deviations and means of the shear force $T_X$, acting in direction $X$, at the tower base as function of $\Phi_y$ and $k$ (device yield force and stiffness, respectively)

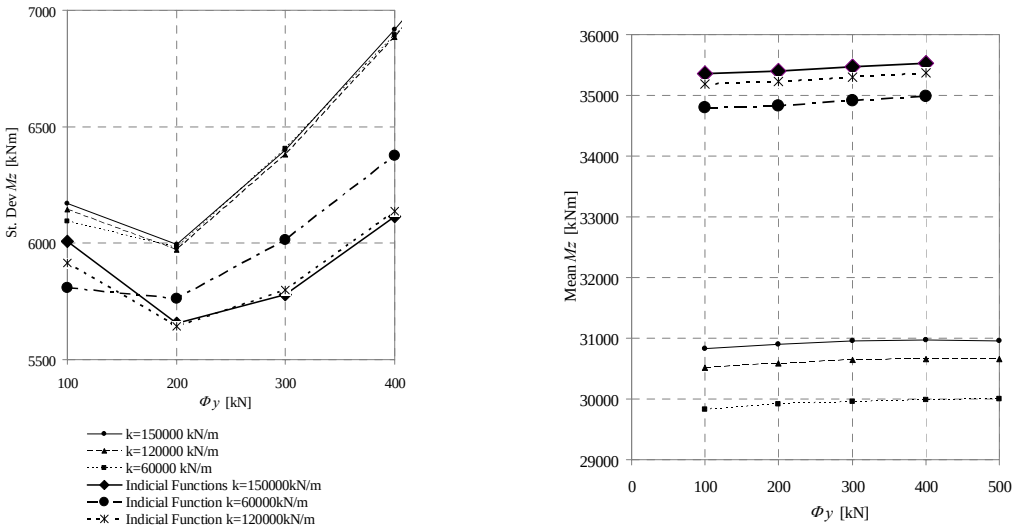


Fig. 8 Standard deviations and means of the bending moment $M_Z$, acting along direction $Z$, at the tower base as function of $\Phi_y$ and $k$ (device yield force and stiffness, respectively)

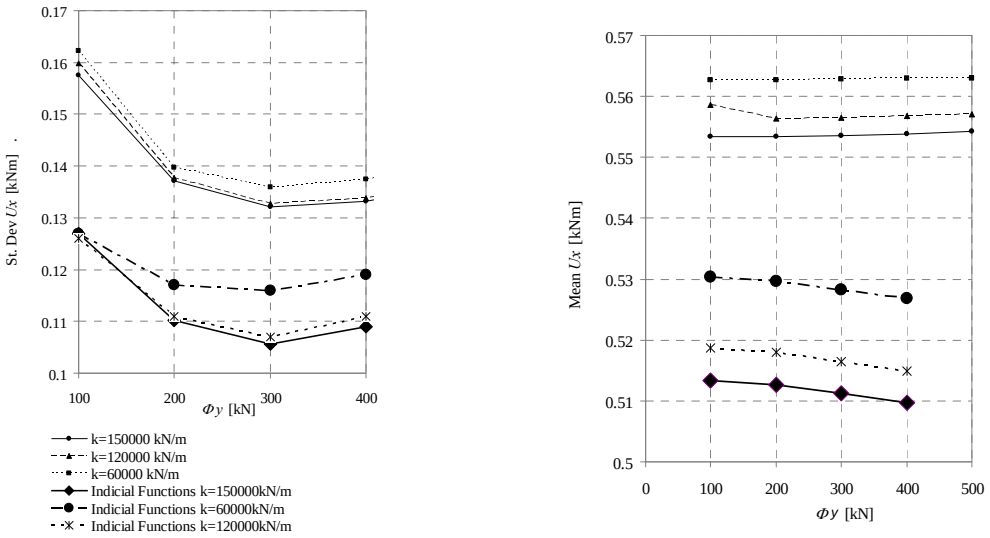


Fig. 9 Standard deviations and means of the displacement $U_X$, in direction $X$, at the deck mid-span as function of $\Phi_y$ and $k$ (device yield force and stiffness, respectively).

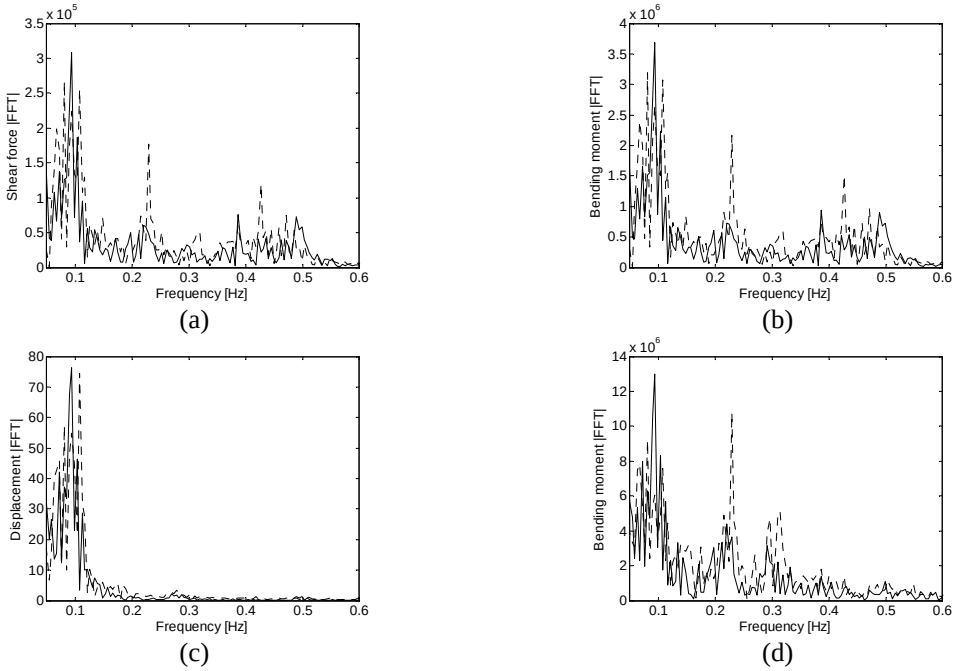


Fig. 10 Frequency domain comparison between the two approaches to wind buffeting (simplified one = point lines, indicial functions = solid line): base tower shear force $T_X$ (a), base tower bending moment $M_Z$ (b), mid-span displacement $U_X$ (c), quarter-span bending moment $M_Y$ (d)

Table 5 Comparison in terms of mean, standard deviation and maximum intensity values, for the optimal passive control systems, between the two considered approaches to buffeting forces

| | **Quasi-static** | | | **Indicial Functions** | | |
|---|---|---|---|---|---|---|
| | *Mean* | *Standard Dev.* | *Max* | *Mean* | *Standard Dev.* | *Max* |
| *Tower base* $F_X$ *[kN]* | -3870 | 530 | -5998 | -4250 | 482 | -5543 |
| *Tower base* $M_Z$ *[kNm]* | 30960 | 6400 | 56419 | 35470 | 5798 | 51107 |
| *Mid-span* $U_X$ *[m]* | 0.55 | 0.13 | 0.93 | 0.51 | 0.10 | 0.79 |
| *Mid-span* $M_Y$ *[kNm]* | 163180 | 44990 | 269700 | 142660 | 32430 | 234700 |
| *Quart.-span* $M_Y$ *[kNm]* | 74380 | 21110 | 173200 | 72280 | 13380 | 155500 |

Table 6 Mean and standard deviation values of the cross-section displacement along global axis $X$ and rotation around global axis $Z$ at the quarters and the middle of the bridge span ($L$)

| *Position* | *1/4L* | *3/4L* | *1/4L* |
|---|---|---|---|
| | Displacement along $X$ [m] | | |
| *Mean* | 0.521 | 0.390 | 0.386 |
| *Standard D.* | 0.0995 | 0.0699 | 0.0700 |
| | Rotation about $Z$ [rad] | | |
| *Mean* | -0.00042 | -0.00085 | -0.00074 |
| *Standard D.* | 0.00011 | 0.00016 | 0.00014 |

The curves associated to the more refined version of the interaction forces (continuous lines in Fig. 10) show generally higher amplitudes at the frequency of the main lateral symmetric mode (see also Table 2). Conversely, when the bridge implements the simplified approach of wind buffeting, it experiences larger amplitudes at higher frequencies, associated to vertical–modal shapes.

Table 6 reports the mean and standard deviation values of the deck vibration displacements in direction $X$ and rotations around its longitudinal axis $Z$ at the quarters and at the middle of the span when the more refined version of the interaction forces is implemented. The vertical displacements $Y$ are not shown since they undergo a very small variation. The rotational components show very small amplitude, confirming the positive outcomes of the numerical analyses with the simpler model for the aerodynamic forces. This result can be traced to the aerodynamic stability characteristics of the bridge cross-section, designed not to undergo flutter phenomena for velocities well over the one adopted in this study.

The wind velocity inducing flutter instability has been evaluated with the refined model of the wind interaction forces for the uncontrolled bridge version and the passive controlled one. From the numerical analyses it has been identified at 134.6 m/s for both the bridge configurations and, consequently, no stability benefit on the Shimotsui-Seto bridge can be gained from the proposed control systems.

This result could have been foreseen by observing the devices implementation in the horizontal

plane, which do not influence the “as built” torsional stiffness of the bridge deck and hence its critical flutter velocity. Furthermore, owing to the large dimensions of the structure, and, therefore, its high flexibility, the exchanged control forces between the deck and the towers, quite far from the center span, are not able to improve the already good original flutter stability.

## 5. Conclusions

A reevaluation of a previously developed strategy for the optimization, under wind excitation, of a passive damping system based on linear devices connecting the deck and the towers, is here studied within a more refined representation of the fluid interaction forces on the Shimotsui-Seto Bridge.

The results obtained, adopting for the deck a representation based on indicial function for the lift and moment components, do not change the outcomes already attained through a simplified model of the buffeting wind forces which considers drag components only. This is due both to the well-designed aerodynamic shape of the deck, which avoids high values of the aerodynamic moments in the deck for small angles of attack, and to the high torsional and vertical stiffness of the same which provide very low deformability and, consequently, largely diminish the contribute to the angle of incidence due to twist and vertical motion of the deck.

The passive control arrangement, already previously identified as the optimal one with the simplified model of wind interaction forces, still achieves the best compromise between the reduction of internal forces and the displacements.

Standard deviation and mean values of the internal forces at the towers base and displacements at mid-span of the girder have been considered as objective functions for the optimization process of the passive control system. Comparing the resulting curves of the selected objective functions versus the device yielding force and stiffness, when the simplified and the refined wind loading simulation is employed, the following observations also arise:

- the optimal configuration, which minimizes one selected objective function, does not in general minimize also the other ones. In other words, the optimal arrangement for the control system comes at the cost of a lower performance for some other structural aspects. However, the values for the device parameters that correspond to the minimum of each individual objective function belong to a small sub-domain of the parameters space.
- The simplified wind loading model leads to an overestimation of the standard deviation of the objective functions, an in general of the extreme values, with respect to the results obtained with the more refined approach based on the use of indicial functions.

This conclusions, that suggest it is conservative to design the control system with reference to the quasi-steady representation of the wind forces, can be of interest in the design of optimal control strategies on long span suspension bridges, owing to the simplification in the implementation of the wind interaction forces.

## Acknowledgements

This work has been partially supported by MIUR (Ministry of Education, University and Research) under the project “Dynamic response of linear and nonlinear structures: modeling,

testing and identification" (PRIN 2009). The support of this work by Mr. Masahiro Nishitani – Honshu-Shikoku Bridge Expressway Company, Japan – is gratefully acknowledged also.

## References

Allemang, R.J. and Brown, D.L. (1982), "A correlation coefficient for modal vector analysis", *Proceedings of the 1st Inter-national Modal Analysis Conference (IMAC)*.

ANSYS ACADEMIC RESEARCH, v. 11.0, *Ansys Inc*., Canonsburg, PA, United States.

Borri, C. and Höffer, R. (2000), "Aeroelastic wind forces on flexible bridge girders", *Meccanica*, **35**(1), 1-15.

Caracoglia, L. and Jones, N.P. (2003), "Time domain vs. frequency domain characterization of aeroelastic forces for bridge deck sections", *J. Wind Eng. Ind. Aerod.*, **91**(3), 371-402.

Casciati, F. and Domaneschi, M. (2007), "Semi-active electro-inductive devices: characterization and modelling", *J. Vib.Control.*, **13**(6), 815-838.

Chen, X. and Kareem, A. (2001), "Nonlinear response analysis of long-span bridges under turbulent winds", *J. Wind Eng. Ind. Aerod*., **89**(14-15), 1335-1350.

Chen, X. and Kareem, A. (2003), "Aeroelastic analysis of bridges: effects of turbulence and aerodynamic nonlinearities", *J. Eng. Mech. - ASCE*, **129**(8), 885-895.

Chen, X., Matsumoto, M., Kareem, A. (2000) ,"Time domain flutter and buffeting response analysis of bridges", *J. Eng. Mech. - ASCE*, **126**(1), 7-16.

CNR-DT 207 (2008), *Instructions for the wind effects and actions evaluations on buildings* , (in Italian).

Domaneschi, M. (2010), "Feasible control of the ASCE benchmark cable-stayed bridge", *Struct. Control. Health. Monit*., **17**(6), 675-693.

Domaneschi, M. (2012), "Simulation of controlled hysteresis by the semi-active Bouc-Wen Model", *Comput. Struct.*, **106-107**, 245-257.

Domaneschi, M. and Martinelli, L. (2009), "Mitigation of the wind buffeting on a suspended bridge by smart devices", *Proceedings of the 5th European & African Conference on Wind Engineering (EACWE 5)*, Florence, Italy.

Domaneschi, M. and Martinelli, L. (2011), "Fatigue mitigation in a long span suspension bridge with a steel frame deck", *Proceedings of the 13th International Conference on Civil, Structural and Environmental Engineering Computing (CC2011)*, Chania, Crete, Greece.

Domaneschi, M. and Martinelli, L. (2012), "Performance comparison of passive control schemes for the numerically improved ASCE cable-stayed bridge model", *Earthq. Struct.*, **3**(2), 181-201.

Domaneschi, M. and Martinelli, L. (2013), "Optimal passive and semi-active control of a wind excited suspension bridge", *Struct. Infrastruct. E.*, **9**(3), 242-259.

Domaneschi, M., Martinelli, L. and Romano. M. (2010), "A strategy for modelling external user element in ANSYS: the Bouc-Wen and the Skyhook case", *Proceedings of the 34th IABSE Symposium 2010*, Venice, Italy.

Erlicher, S. and Point, N. (2004), "Thermodynamic admissibility of Bouc-Wen type hysteresis models", *CR Mecanique*, **332**(1), 51-57.

Engineering Sciences Data Unit (1988), *Lattice structures Part 1: mean fluid forces on single and multiple plane frames*, ESDU 81027, Wind Engineering Sub-Series, ESDU International, London.

Engineering Sciences Data Unit (1971), *Fluid forces on non-streamline bodies - background notes and description of the flow phenomena*, ESDU 71012, Wind Engineering Sub-Series, ESDU International, London.

Eurocode 1 - UNI EN 1991-1-4 (2005), "Actions on structures - Part 1-4: General actions - wind actions".

Garcia, D.L. and Soong, T.T. (2002), "Efficiency of a simple approach to damper allocation in MDOF structures", *J. Struct.Control.*, **9**(1), 19-30.

Hao, H., Oliveira, C.S. and Penzien, J. (1989), "Multiple-station ground motion processing and simulation

based on SMART-1 array data", *Nucl. Eng. Des*., **111**(3), 293-310.
Ikhouane, F., Manosa, V. and Rodellar, J. (2007a), "Dynamic properties of the hysteretic Bouc-Wen model", *Syst. Control. Lett.*, **56**(3), 197-205.
Ikhouane, F., Hurtado, J.E. and Rodellar, J. (2007b), "Variation of the hysteresis loop with the Bouc–Wen model parameters", *Nonlinear. Dynam*., **48**(4), 361-380.
Ismail, M., Ikhouane, F. and Rodellar, J. (2009), "The hysteresis bouc-wen model, a survey", *Arch. Comput. Method. E*., **16**(2), 161-188.
Kitagawa, M. (2004), "Technology of the Akashi Kaikyo Bridge", *Struct. Control. Health. Monit*., **11**(2), 75-90.
Leishman, J.G. (2000), *Principles of helicopter aerodynamics*, Cambridge Univ. Press.
Low, T.S. and Guo, W. (1995), "Modeling of' a three-layer piezoelectric bimorph beam with hysteresis", *J Microelectromech. S.*, **4**(4), 230-237.
Martinelli, L. and Perotti, F. (2001), "Numerical Analysis of the non-linear dynamic behaviour of suspended cables under turbulent wind excitation", *Int. J. Struct. Stab. Dyn.*, **1**(2), 207-233.
Pareto, V. (1927), Manuel d'économie Politique, Giard, Paris.
Romano, M. (2009), *Ponti Sospesi: Controllo sotto azioni eoliche*, MSc Thesis (in Italian), Politecnico di Milano, Milan, Italy.
Salvatori, L. and Borri, C. (2007), "Frequency- and time-domain methods for the numerical modeling of full-bridge aeroelasticity", *Comput. Struct.*, **85**(11-14), 675-687.
Salvatori, L. and Spinelli, P. (2006), "Effects of structural nonlinearity and along-span wind coherence on suspension bridge aerodynamics: some numerical simulation results", *J. Wind Eng. Ind. Aerod*., **94**(5), 415-430.
Scanlan, R.H., Beliveau, J.G., Budlong, K.S. (1974), "Indicial aerodynamic function for bridge decks", *J. Eng. Mech. - ASCE*, **100**(4), 657-672.
Solari, G. and Piccardo, G. (2001), "Probabilistic 3-D turbulence modeling for gust buffeting of structures", *Probabilist. Eng. Mech.*, **16**, 73-86.
Spencer, B.F. Jr, Dyke, S.J., Sain, M.K. and Carlson, J.D. (1997), "Phenomenological model for magnetorheological dampers", *J. Eng. Mech. - ASCE*, **123**, 230-238.
Stoyanoff, S. (2001), "A unified approach for 3D stability and time domain response analysis with application of quasi-steady theory", *J. Wind Eng. Ind. Aerod.*, **89**(14-15), 1591-1606.
Ubertini, F. (2011), "Prevention of suspension bridge flutter using multiple tuned mass dampers", *Wind Struct*., **13**(3), 235-256.
Wen, Y.K. (1976), "Method for random vibration of hysteretic systems", *J. Eng. Mech.- ASCE*, **102**(2), 249-263.
Zhang, R.H. and Soong, T.T. (1992), "Seismic dsign of viscoelastic dmpers for sructural aplications", *J. Struct. Eng. - ASCE*, **118**(5), 1375-1392.
Zhang, Z., Chen, Z., Cai, Y. and Ge, Y. (2011), "Indicial functions for bridge aeroelastic forces and time-domain flutter analysis", *J. Bridge Eng. - ASCE*, **16**(4), 546-557.

*JH*